Asymmetric Bound States of Spiral Pairs in Excitable Media

Christian Zemlin,[1] Karthik Mukund,[1] Marcel Wellner,[1] Roman Zaritsky,[2] and Arkady Pertsov[1]
[1]*Department of Pharmacology, SUNY Upstate Medical University, Syracuse, New York 13210, USA*
[2]*Department of Computer Science, Montclair State University, Upper Montclair, New Jersey 07043, USA*
(Received 3 March 2005; published 26 August 2005)

We present a stable regime of asymmetric bound states for spiral pairs in a generic numerical model of a homogeneous excitable medium. In this regime, one spiral tip (slave) rotates around the other (master). Master-slave dynamics occur for both same-chirality and opposite-chirality spiral pairs in a range of parameters and initial conditions. We study the dependency of master-slave characteristics on the medium's excitation threshold and present a phenomenological model that accounts for the qualitative properties of master-slave dynamics.

DOI: 10.1103/PhysRevLett.95.098302 PACS numbers: 82.40.Ck, 05.65.+b, 89.75.Kd

Spiral waves in excitable media are a remarkable example of self-organization. They have been observed in the Belousov-Zhabotinsky reaction [1,2], electrical activity in cardiac tissue [3], aggregation of starving slime mold amoeba [4], and catalytic reactions on platinum surfaces [5].

Intriguing analogies have emerged between spiral waves and particles. The most obvious analogous feature is narrow localization in space: In this Letter, as well as in much of the literature, the spatial coordinate of a spiral is taken to be that of its wave front's tip. This definition allows one to speak of spiral-spiral interactions in particlelike terms. Bound states of spiral waves have characteristic features, like their wave emission frequency [6,7], and rules of interaction with other bound states [7].

Two kinds of bound spiral pairs may be distinguished according to their components' chiralities. If both spirals have the same chirality (a state of topological charge ± 2) the system is seen at asymptotic distances from the cores as a single double-armed spiral. If the chiralities are opposite (topological charge zero), we only see concentric circular waves at large distances.

All bound states of spiral pairs reported so far exhibit either axial symmetry (for opposite-chirality pairs) or point symmetry (for same-chirality pairs). Axially symmetric pairs have been observed in virtually every known excitable medium [8,9], most importantly in the heart [10], where they are known as figure-of-eight reentry. Point symmetric pairs, also known as double-armed spirals, spontaneously occur in dictyostelium discoideum [11] and a variety of numerical models [12]; they have been induced in the Belousov-Zhabotinsky reaction [6,13], as well as in the rabbit heart [14] and in two-dimensional cultured heart tissue [15].

Here we report the first observation of stable bound spiral pairs with broken symmetry in a homogeneous excitable medium. The interspiral distance can exceed both the wavelength and the core size of a single spiral wave. A striking feature of these asymmetric bound pairs is that one spiral ("master") is almost unaffected by the other, while the dynamics of the other ("slave") are radically altered by the interaction. By modifying the medium's excitability, we can break and recover symmetry, and we observe hysteresis in the dependency of the system's symmetry on the medium's excitability.

All observations were made in numerical simulations using the Barkley reaction-diffusion model [16] of a generic excitable medium. It consists of an activator variable u and an inhibitor variable v, which evolve according to

$$\begin{aligned} \partial u/\partial t &= (q/\varepsilon)u(1-u)[u-(v+b)/a] + \nabla^2 u, \\ \partial v/\partial t &= u - v. \end{aligned} \tag{1}$$

The constant ε is the ratio of characteristic time scales of the activator and inhibitor variables. The parameters a and b represent the slope of the u nullcline and the excitation threshold.

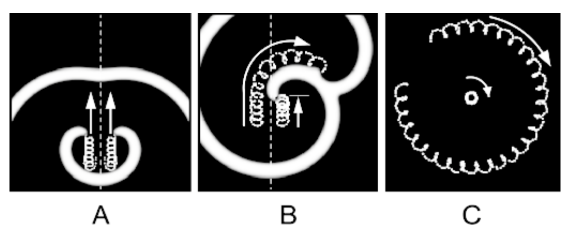

FIG. 1. Spontaneous breaking of axial symmetry and formation of an asymmetric bound state ($b = 0.2135$). Thick white lines show the excitation waves ($u \approx 1$); thin white lines show the tip trajectories. Arrows indicate the drift direction of the tips. Dashed line is the axis of symmetry. (a) Axially symmetric spiral pair before perturbation. (b) Spontaneous symmetry breaking after the medium was perturbed in one pixel. Tip trajectories are continued from panel (a). View is slightly zoomed and centered on the right spiral tip. (c) Steady state spiral tip trajectories [same view as panel (b)]. One spiral (master) is rotating almost unaffected by the other (at the center of the panel), while the other spiral (slave) precesses around the master. The master-slave distance significantly exceeds the core radius of an isolated spiral in the same medium.

We solved the model equations on a 320×320 or 640×640 grid using Euler's method with zero-flux boundary conditions and space and time steps $dx = 0.1826$ and $dt = 0.003$. We chose typical values $\varepsilon = 0.02$ and $a = 1.1$, and varied b. All computations were performed on a 32-node Beowulf cluster. We created same-chirality and opposite-chirality spiral pairs using established methods [17], and defined spiral tips to be pixels satisfying $0.45 < u < 0.57$ and $0 < du/dt < 10$.

Figure 1 shows the symmetry breaking of an opposite-chirality pair and the resulting asymmetric bound state, caused by a small one-time perturbation (lasting one time step). Before the perturbation [Fig. 1(a)], the spiral arms drifted linearly in perfect symmetry. At the instant shown in Fig. 1(a), we set the activator variable at one pixel at the right wave tip to zero. This immediately triggered a breaking of symmetry, shown in Fig. 1(b). The upward motion of the right spiral tip slowed down while the left spiral tip started to drift away from the right tip in a spiral fashion (no picture shown), until it stabilized at a larger distance [see Fig. 1(c)]. The same phenomenon occurred for a variety of small perturbations located sufficiently close to the spiral's tip.

A close inspection revealed that the radius of the inner spiral's core was modulated, with the frequency at which the outer spiral revolved; thus the trajectory in Fig. 1(c) appears thicker. Both tip trajectories can be described as a combination of a simple spiral rotation (as that of a single-armed spiral in the same medium) and a low-frequency precession, caused by the interaction. The two precessions are characterized by the precession radii r_1 and r_2 (with the convention $r_1 > r_2$).

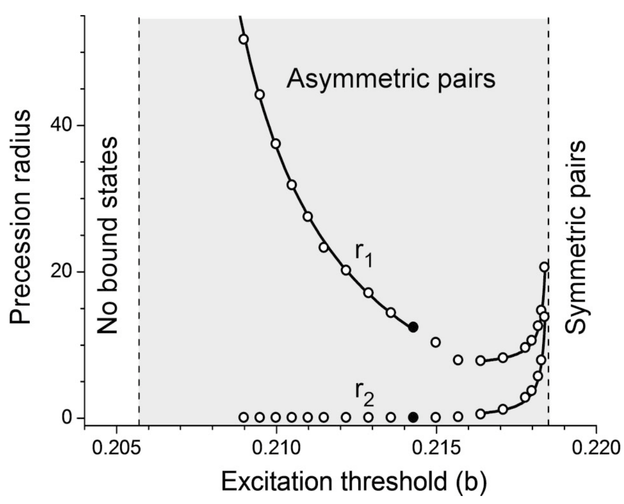

FIG. 2. Characteristics of spiral pairs with opposite chirality at different excitation thresholds (b). The gray area marks the range of b that supports asymmetric bound states. Circles (○) show the radii of precession of the master (r_2) and the slave (r_1). The filled circles correspond to the simulation shown in Fig. 1(c). The solid lines show fits of the diverging segments of r_1 and r_2 with hyperbolic curves of the form $c_0 + c_1/(b - b_c)$; the dashed lines mark the asymptotes ($b_c = 0.2057$ and $b_c = 0.2185$).

The prominent feature of Fig. 1(c) is the asymmetry of the interaction: The inner spiral is almost unaffected ($r_2 \approx 0$), while the outer spiral precesses strongly (r_1 is large compared to the core radius of an isolated spiral). For $r_2 \approx 0$, we call the unaffected inner spiral the master and the strongly precessing outer spiral the slave; in this situation r_1 can be interpreted as the average master-slave distance.

Figure 2 shows how r_1 and r_2 depend on excitability over the whole range that allows asymmetric bound states. For sufficiently low excitation threshold (b), we observe master-slave pairs with large interspiral distances ($r_1 \gg r_2 \approx 0$). In this range, r_1 diverges as b decreases. A $1/(b - b_c)$ singularity is strongly suggested by the excellent fit shown in Fig. 2. If we increase b, the slave approaches the master while the master remains largely unaffected. When b is increased beyond $b = 0.2158$, r_1 and r_2 both grow to infinity, corresponding to a linearly drifting symmetric pair. Close to the singularity, both r_1 and r_2 are hyperbolic curves with essentially the same asymptote ($b_c = 0.2185$). This reflects the fact that both spirals drift in concentric circles and that their radii are coupled as they grow. Above the singularity, only symmetric pairs are stable.

Same-chirality spiral pairs also exhibit spontaneous symmetry breaking into master-slave pairs (see Fig. 3). Fig. 3(a) shows a snapshot of a point symmetric double-armed spiral, for a parameter b similar to that from Fig. 1. As for the axially symmetric case, we added a minimal perturbation, which triggered symmetry breaking [Fig. 3(b)]. The right tip slows down while the left tip begins to orbit around the right tip. After a transition period, we observed master-slave dynamics [Fig. 3(c)], similar to Fig. 1(c).

Figure 4 shows the bifurcation diagram for same-chirality spiral pairs. As in the axially symmetric case, r_1 diverges as $1/(b - b_c)$, with a very similar location of the singularity. As we increase b, r_1 decreases and r_2 increases until, at $b = 0.223$, they become equal and a transition to point symmetric dynamics occurs.

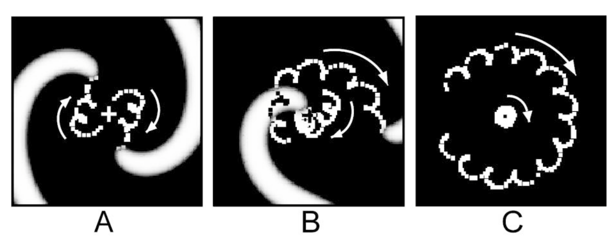

FIG. 3. Spontaneous breaking of point symmetry and formation of an asymmetric bound state ($b = 0.21$). (a) A point symmetric spiral pair. The center of symmetry is marked +. (b) Symmetry breaking after a minimal perturbation. (c) Steady state tip trajectories after symmetry breaking.

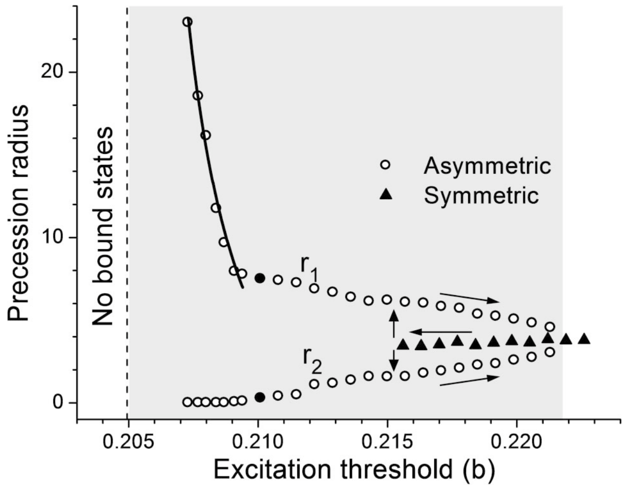

FIG. 4. Bifurcation diagram showing bistability and hysteresis for the dynamics of same-chirality spiral pairs. The gray area marks the range of b that supports asymmetric bound states. Circles (○) show the radii of precession of the master (r_2) and the slave (r_1), triangles (▲) the common average precession radius for the symmetric state. Black arrows indicate which stable branch the system follows if b is increased or decreased. The solid line shows a fit of the diverging segment of r_1 with a hyperbolic curve (as in Fig. 2), and the dashed line marks the corresponding asymptote ($b_c = 0.2049$). The filled circles correspond to the simulation shown in Fig. 3.

It is interesting that for the same-chirality case, there is a broad range of parameters where both symmetric and asymmetric pairs are stable ($0.216 < b < 0.223$). In this parameter range, we observed hysteresis. Indeed, if we start with a symmetric pair and gradually decrease b, symmetric dynamics persist until $b = 0.216$; afterwards, an abrupt transition to master-slave dynamics occurs.

Figure 5 illustrates the transitions between stable asymmetric and symmetric states following abrupt changes in b. A system in the master-slave regime [Fig. 5(a)] switches to axial symmetry with linear drift [Fig. 5(b)] as soon as we increase b, and it returns to master-slave dynamics as soon as the original value of b is restored [Fig. 5(c)]. Note that master and slave have switched roles from Fig. 5(a) to 5(c); in general, which spiral becomes the master and which becomes the slave depends on minimal asymmetries in the initial conditions.

We conducted several tests to assess the robustness of master-slave pairs. We tested the sensitivity to initial conditions, including initial conditions that can be reproduced experimentally ("vortex shedding" [18]). We furthermore applied one-time global perturbations of varying amplitude and spatial frequency and, in separate simulations, continuously added random noise. All these tests demonstrated the robustness of master-slave pairs. The pairs persisted up to considerable perturbation amplitudes (90% of the excitation threshold for one-time perturbations, 7.5% for continuously added random noise). Medium size and boundary conditions were relevant only if the slave got close to the boundary.

The mechanisms by which master-slave pairs are formed and sustained can be understood qualitatively with the following considerations. Master-slave pairs form after the symmetry breaking induces a difference in the rotation frequencies of the spirals; the faster spiral becomes the master. The subsequent dynamics can be described in terms of induced drift, which has been reported for spiral waves exposed to a train of plane waves [8,19,20]. The fact that the periodic wave train emitted by the master is curved rather than planar causes the slave to drift in a circular rather than linear path and ensures the existence of a stable steady state, as we show below. Figure 6 sketches a simple phenomenological model that accounts for the stability of master-slave pairs and the qualitative dependency of r_1 on b.

The model is based on the following assumptions derived from numerical experiments: The master, whose core center is at C, periodically emits circular wave fronts, which hit the slave tip (S). Between successive hits, the trajectory of S is circular and has the same radius r_s as the core of an isolated spiral. The slave front right after a collision is identical to a section of the incoming master front. The periodic collisions increase the slave's rotation period such that between two successive collisions, it

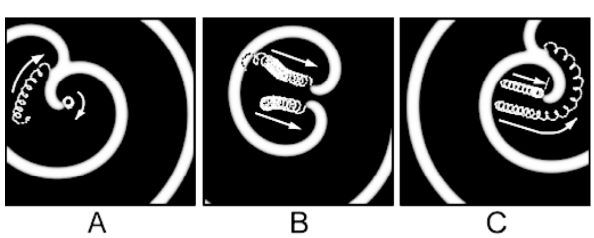

FIG. 5. Reversibility of symmetry breaking. (a) Master-slave pair ($b = 0.2135$). (b) When we change b to 0.22 and continue the simulation, the spiral pair becomes symmetric and starts drifting linearly. (c) After b is set back to 0.2135, symmetry breaks again, turning the system back into a master-slave pair.

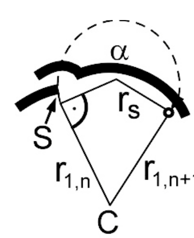

FIG. 6. Evolution of the slave's tip (S). The thick lines show the wave fronts shortly after a collision. At the moment of collision, the distance from S to the center C of the master was $r_{1,n}$. After the collision, the S moves along a circular arc of radius r_s, covering an angle α before colliding with the master again at distance $r_{1,n+1}$.

rotates by an angle α that is typically slightly larger than π [see Fig. 1(c)].

Under these assumptions, the distance $r_{1,n}$ from S to C evolves according to

$$(r_{1,n+1})^2 - (r_{1,n})^2 = 2r_s[r_s(1 + \cos(\alpha - \pi)) - r_{1,n} \sin(\alpha - \pi)]. \quad (2)$$

If we assume that $\alpha - \pi$ is small, take a first-order approximation, and set the left side of Eq. (2) to zero, we obtain the condition for a steady state,

$$r_1 = 2r_s/(\alpha - \pi). \quad (3)$$

A stability analysis of Eq. (2) shows that the steady state is stable.

Equation (3) predicts that r_1 grows as α approaches π from above and has a singularity at $\alpha = \pi$, independent of the relative chirality of master and slave; this is consistent with our numerical simulations. However, the simulations also show that r_1 is consistently larger for opposite-chirality than for same-chirality pairs for a given b (compare Figs. 2 and 4). This difference can be accounted for if the master wave front is taken to be spiral-shaped rather than circular. In this case, an analysis similar to that carried out above for circular master wave fronts predicts r_1 to be larger for opposite-chirality pairs.

Our finding of asymmetric bound states represents a major shift from the common views that there is no long-range interaction between and that in a homogeneous medium, all spirals are equal. In our model system, we can reversibly adjust the spiral pair tip distance or, if we change the excitability beyond the limit of the master-slave domain, switch from asymmetric to symmetric bound states.

Bound states of spirals are a robust phenomenon; it is therefore likely that they can also be observed in experiments. A possible candidate medium is the Belousov-Zhabotinski reaction, in which symmetry breaking of axially symmetric pairs was found [21,22], although it resulted in expulsion of one of the spirals rather than in a bound state. Our results suggest a bound state could have been observed in these experiments if the medium had a higher excitation threshold. It would be interesting to revisit these experiments with our results in mind.

The existence of bound states of spiral waves may have important implications in cardiology. Animal experiments have demonstrated both the presence of multiple rotors during fibrillation [23] and the possibility of inducing double-armed spirals [14] in the mammalian heart. It is therefore not unlikely that bound pairs of spirals occur in the mammalian heart; in this case the best treatment of them becomes an important question.

This work was supported by AHA Grant No. 0325458T, by NIH Grants No. 5R01HL071635 and No. 5R01HL071762, and by NSF Grant No. CTS-0319555. We thank Olivier Bernus and Charles Danko for helpful discussions.

[1] A. N. Zaikin and A. M. Zhabotinsky, Nature (London) **225**, 535 (1970).
[2] A. T. Winfree, Science **175**, 634 (1972).
[3] J. M. Davidenko *et al.*, Nature (London) **355**, 349 (1992).
[4] K. J. Lee, E. C. Cox, and R. E. Goldstein, Phys. Rev. Lett. **76**, 1174 (1996).
[5] M. Bär, I. G. Kevrekidis, H. H. Rotermund, and G. Ertl, Phys. Rev. E **52**, R5739 (1995).
[6] K. I. Agladze and V. I. Krinsky, Nature (London) **296**, 424 (1982).
[7] R. M. Zaritski and A. M. Pertsov, Phys. Rev. E **66**, 066120 (2002).
[8] V. I. Krinsky and K. I. Agladze, Physica (Amsterdam) **D8**, 50 (1983).
[9] K. Asakura, J. Lauterbach, H. H. Rotermund, and G. Ertl, Phys. Rev. B **50**, 8043 (1994).
[10] I. Banville, R. A. Gray, R. E. Ideker, and W. M. Smith, Circ. Res. **85**, 742 (1999).
[11] B. Vasiev, F. Siegert, and C. Weijer, Phys. Rev. Lett. **78**, 2489 (1997).
[12] R. Zaritski, J. Ju, and I. Ashkenazi, Int. J. Bifurcation Chaos Appl. Sci. Eng. (to be published).
[13] O. Steinbock and S. C. Müller, Int. J. Bifurcation Chaos Appl. Sci. Eng. **3**, 437 (1993).
[14] T. J. Wu, M. A. Bray, C. T. Ting, and S. F. Lin, J. Cardiovasc. Electrophysiol. **13**, 414 (2002).
[15] N. Bursac, F. Aguel, and L. Tung, Proc. Natl. Acad. Sci. U.S.A. **101**, 15530 (2004).
[16] D. Barkley, M. Kness, and L. S. Tuckerman, Phys. Rev. A **42**, 2489 (1990).
[17] E. A. Ermakova, A. M. Pertsov, and E. E. Shnol, Physica (Amsterdam) **D40**, 185 (1989).
[18] C. Cabo *et al.*, Biophys. J. **70**, 1105 (1996).
[19] E. A. Ermakova, V. I. Krinsky, A. V. Panfilov, and A. M. Pertsov, Biophysics **31**, 348 (1986).
[20] G. Gottwald, A. Pumir, and V. I. Krinsky, Chaos **11**, 487 (2001).
[21] M. Ruiz-Villarreal *et al.*, Phys. Rev. E **54**, 2999 (1996).
[22] H. Brandtstädter, M. Braune, I. Schebesch, and H. Engel, Chem. Phys. Lett. **323**, 145 (2000).
[23] R. A. Gray, A. M. Pertsov, and J. Jalife, Nature (London) **392**, 75 (1998).